Surface-Functionalized Polymeric Nanoparticles as Templates for Biomimetic Mineralization of Hydroxyapatite

Anitha Ethirajan,[†,‡] Ulrich Ziener,[†] and Katharina Landfester*[,†,‡]

Institute of Organic Chemistry III (Macromolecular Chemistry and Organic Materials), University of Ulm, Albert-Einstein-Allee 11, D-89081 Ulm, Germany, and Max Planck Institute for Polymer Research, Ackermannweg 10, D-55128 Mainz, Germany

Received January 19, 2009. Revised Manuscript Received March 10, 2009

The use of polymeric nanoparticles as templates for producing inorganic materials is an intriguing approach, as it offers the feasibility of synthesizing organic/inorganic hybrid materials for several interesting applications. Here, polymeric nanoparticles synthesized via the miniemulsion process are employed as templates for biomimetic mineralization of hydroxyapatite in the aqueous phase. The versatile miniemulsion technique allows the fabrication of surface-functionalized polymeric nanoparticles with varying amounts of surface-bound functional groups by use of different types of surfactants. Hybrid nanoparticles were formed by performing crystallization outside on the surface of the polymer nanoparticles by varying the amount of surface functional groups and were studied by high-resolution scanning electron microscopy (HRSEM), transmission electron microscopy (TEM), and X-ray diffraction (XRD). These hydroxyapatite/polymer hybrid nanoparticles have great potential to be used as filler or as scaffold for nucleation and growth of new bone material. They offer the feasibility of being injected directly into the damaged part in addition to being applied as coatings on implants. The use of polymeric nanoparticles coated with hydroxyapatite (HAP) for bone repair applications in addition opens new doors for realizing the potential of using the polymeric nanoparticles as carriers of drugs and growth factors to better treat bone defects and promote wound healing.

Introduction

The use of polymeric nanoparticles as templates for the crystallization of inorganic materials is an intriguing approach, as it offers the feasibility of synthesizing organic/inorganic hybrid materials for a broad spectrum of applications.[1,2] Organic templates employing surfactant assemblies,[3−5] hydrogels,[6,7] block copolymers,[8,9] polyelectrolytes,[10] self-associated nanogels,[11] emulsions, and microemulsions[12−14] have already been exploited for synthesizing inorganic materials, for example, calcium phosphates. Other interesting biomimetic routes for the mineralization of calcium phosphates (apatites) employing biodegradable synthetic polymers,[15,16] collagen,[17,18] and gelatin[19,20] are well-known in the literature. Recently, we have reported a biomimetic approach to synthesize gelatin/hydroxyapatite hybrid nanoparticles using gelatin nanoparticles synthesized via the miniemulsion technique as templates.[21,22] The possibility to control structure, shape, and size has made the biomimetic approaches very fascinating.[23] Synthesis of hybrid particles by the encapsulation of preformed inorganic materials within a polymeric matrix has also been reported.[24] However, the in situ formation of inorganic materials allows the variation of several parameters and offers better organic/inorganic interface integrity. As compatibility of the inorganic component with the organic matrix plays a crucial role for encapsulation

* To whom correspondence should be addressed: tel +49 6131 379-171; fax +49 6131 379-370; e-mail landfester@mpip-mainz.mpg.de.
† University of Ulm.
‡ Max Planck Institute for Polymer Research.

(1) Zhang, J. G.; Xu, S. Q.; Kumacheva, E. *J. Am. Chem. Soc.* **2004**, *126*, 7908.
(2) Hain, J.; Pich, A.; Adler, H.-J. P. *Macromol. Symp.* **2007**, *254*, 128.
(3) Welzel, T.; Meyer-Zaika, W.; Epple, M. *Chem. Commun.* **2004**, *10*, 1204.
(4) Fowler, C. E.; Li, M.; Mann, S.; Margolis, H. C. *J. Mater. Chem.* **2005**, *15*, 3317.
(5) Sarda, S.; Heughebaert, M.; Lebugle, A. *Chem. Mater.* **1999**, *11*, 2722.
(6) Schnepp, Z. A. C.; Gonzalez-McQuire, R.; Mann, S. *Adv. Mater.* **2006**, *18*, 1869.
(7) Schachschal, S.; Pich, A.; Adler, H.-J. *Langmuir* **2008**, *24*, 5129.
(8) Antonietti, M.; Breulmann, M.; Göltner, C. G.; Cölfen, H.; Wong, K. K. W.; Walsh, D.; Mann, S. *Chem.—Eur. J.* **1998**, *4*, 2493.
(9) Kakizawa, Y.; Miyata, K.; Furukawa, S.; Kataoka, K. *Adv. Mater.* **2004**, *16*, 699.
(10) Shchukin, D. G.; Sukhorukov, G. B.; Möhwald, H. *Angew. Chem., Int. Ed.* **2003**, *42*, 4472.
(11) Sugawara, A.; Yamane, S.; Akiyoshi, K. *Macromol. Rapid Commun.* **2006**, *27*, 441.
(12) Lim, G. K.; Wang, J.; Ng, S. C.; Gan, L. M. *Langmuir* **1999**, *15*, 7472.
(13) Walsh, D.; Hopwood, J. D.; Mann, S. *Science* **1994**, *264*, 1576.
(14) Perkin, K. K.; Turner, J. L.; Wooley, K. L.; Mann, S. *Nano Lett.* **2005**, *5*, 1457.
(15) Rezwan, K.; Chen, Q. Z.; Blaker, J. J.; Boccaccini, A. R. *Biomaterials* **2006**, *27*, 3413.
(16) Kretlow, J. D.; Mikos, A. G. *Tissue Eng.* **2007**, *13*, 927.
(17) Bradt, J.-H.; Mertig, M.; Teresiak, A.; Pompe, W. *Chem. Mater.* **1999**, *11*, 2694.
(18) Olszta, M. J.; Cheng, X. G.; Jee, S. S.; Kumar, R.; Kim, Y. Y.; Kaufman, M. J.; Douglas, E. P.; Gower, L. B. *Mater. Sci. Eng., R* **2007**, *58*, 77.
(19) Rosseeva, E. V.; Buder, J.; Simon, P.; Schwarz, U.; Frank-Kamenetskaya, O. V.; Kniep, R. *Chem. Mater.* **2008**, *20*, 6003.
(20) Bigi, A.; Panzavolta, S.; Rubini, K. *Chem. Mater.* **2004**, *16*, 3740.
(21) Ethirajan, A.; Schoeller, K.; Musyanovych, A.; Ziener, U.; Landfester, K. *Biomacromolecules* **2008**, *9*, 2383.
(22) Ethirajan, A.; Ziener, U.; Chuvilin, A.; Kaiser, U.; Cölfen, H.; Landfester, K. *Adv. Funct. Mater.* **2008**, *18*, 2221.
(23) Xu, A.-W.; Yurong, M.; Cölfen, H. *J. Mater. Chem.* **2007**, *17*, 415.
(24) Qiu, X.; Han, Y.; Zhuang, X.; Chen, X.; Li, Y.; Jing, X. *J. Nanopart. Res.* **2007**, *9*, 901.

10.1021/cm9001724 CCC: $40.75 © 2009 American Chemical Society
Published on Web 05/01/2009

efficiency, very often an additional coating of the inorganic material with a polymer or a surfactant (in this case as a surface modifier as well as to separate individual entities to ease encapsulation) is a prerequisite. Moreover, the inorganic component is encapsulated very often within the matrix. For applications involving the inorganic materials outside the nanoparticle matrix, the synthetic possibilities are very much limited.

Surface-functionalized nanoparticles are very good candidates to serve as templates to perform crystallization outside on the surface of the particles, owing to their monodisperse size and large surface area. The usage of such nanoparticles for biomimetic hydroxyapatite (HAP) deposition is interesting for applications involving bioimplants. For example, implants made of titanium and its alloys can be coated with HAP in order to eliminate the failure of the implant owing to poor osteoconductive properties and to impart better osteointegration and bonding between implant and bone.[25−27] In order to take advantage of the biocompatibility of HAP as well as the mechanical properties of the underlying metallic substrate, it is necessary to optimize the coating possibilities of implants with complex shapes. One of the excellent options to enhance the surface coating possibilities is to use HAP-coated nanoparticles. The presence of HAP on the surface of the nanoparticles offers several advantages: it allows the implant material to adapt to the surrounding tissues; it can act as a scaffold for nucleation and growth of new bone materials; and it can impart nanoscaled features on the surface, thereby modifying the surface topography and influencing the physicochemical properties as well as the biochemistry at the surface.[28] Above all, a valuable aspect is that these nanoparticles in addition can also act as carriers of biomolecules and drugs.

Surface-functionalized nanoparticles can be very well exploited as templates for the growth of hydroxyapatite crystals on the polymeric nanoparticle surface. Tamai and Yasuda[29] have reported HAP-coated polymer particles by employing Pd^0 immobilized poly(styrene-*co*-acrylic acid) copolymer particles synthesized via emulsifier-free emulsion polymerization. Later, the formation of HAP nanocrystals on the surface of β-diketone-functionalized polymeric nanoparticles employing styrene and acetoacetoxyethyl methacrylate (AAEM) obtained by emulsifier-free emulsion polymerization have been reported.[30] The carboxylated polystyrene latex particles have also been used previously for the preparation of other inorganic materials like Ag/AgO.[31] However, in these above-mentioned studies the amount of functional groups was always fixed and the amount of inorganic material precipitated was controlled by controlling either the reaction parameters[29,31] or the amount of added respective salts.[30] The synthesis of functionalized polystyrene particles by miniemulsion polymerization has been well-studied and documented.[32] The miniemulsion technique allows the synthesis of amino- or carboxyl-functionalized polystyrene particles with different amounts of bound surface charge groups by varying the amount of functional comonomer, acrylic acid.[32,33]

In the previous studies that used self-assembled monolayers (SAMs) with several functional groups (-OH, $-SO_3H$, $-PO_4H_2$, -COOH) on Ti wafers, the -COOH functional group has been proven to be an optimal end group for producing highly crystalline and thick layers of HAP.[34] Thus, the usage of carboxyl-functionalized polystyrene particles synthesized via the miniemulsion polymerization as templates seems to be a practical way to synthesize hybrid colloids with highly crystalline HAP. These hybrid particles could be finally used for the coating of implants in order to make them more osteoconductive as well as for the preparation of scaffolds for tissue engineering. It is the aim of this work to use surface-functionalized particles with covalently bound carboxyl groups, which were prepared by use of an ionic as well as a nonionic surfactant as template to perform crystallization on the surface of the particles. This approach of crystallization outside the particle is in contrast to our previous report,[22] where the crystallization was performed inside gelatin nanoparticles, which served as a confined reaction environment. Here, the influence of the type of surfactant with respect to particle size, density of functional surface groups, and HAP formation were studied in detail. The hybrid particles were characterized by high-resolution scanning electron microscopy (HRSEM), transmission electron microscopy (TEM), and X-ray diffraction (XRD).

Experimental Section

Materials. Styrene (Merck) and acrylic acid (Aldrich) were freshly distilled under reduced pressure and stored at −20 °C before use. All other chemicals were used without further purification: the hydrophobic monomer-soluble initiator 2,2′-azobis(2-methylbutyronitrile) (V59) from Wako Chemicals, Japan; the hydrophobe hexadecane (Aldrich, 99%); the nonionic surfactant Lutensol AT50 [a poly(ethylene oxide)-hexadecyl ether with an EO block length of about 50 units] from BASF; and the ionic surfactant sodium dodecyl sulfate (SDS) from Merck. For loading of the particles, calcium nitrate tetrahydrate (Aldrich, 99%) and diammonium hydrogen phosphate (Merck) were used. Demineralized water was used during the experiments.

Synthesis by Direct Miniemulsion. Carboxyl-functionalized polystyrene nanoparticles with ionic as well as nonionic surfactants were prepared by the miniemulsion copolymerization of styrene with varying amounts of the comonomer, acrylic acid. Quantities are given in Table 1. For the preparation of poly(styrene-*co*-acrylic acid) latex particles, the given amount of styrene and acrylic acid, 250 mg of the hydrophobe hexadecane, and 100 mg of the initiator V59 were added to 24 g of water containing 200 mg of Lutensol

(25) Cook, S. D.; Thomas, K. A.; Kay, J. F.; Jarcho, M. *Clin. Orthop. Relat. Res.* **1988**, *232*, 225.
(26) Campbell, A. A.; Fryxell, G. E.; Linehan, J. C.; Graff, G. L. *J. Biomed. Mater. Res.* **1996**, *32*, 111.
(27) Ducheyne, P.; Beight, J.; Cuckler, J.; Evans, B.; Radin, S. *Biomaterials* **1990**, *11*, 531.
(28) Mendonca, G.; Mendonca, D. B. S.; Aragão, F. J. L.; Cooper, L. F. *Biomaterials* **2008**, *29*, 3822.
(29) Tamai, H.; Yasuda, H. *J. Colloid Interface Sci.* **1999**, *212*, 585.
(30) Schachschal, S.; Pich, A.; Adler, H.-J. P. *Colloid Polym. Sci.* **2007**, *285*, 1175.
(31) Zhang, R.; Zhang, D.; Mao, H.; Song, W.; Gao, G.; Liu, F. *J. Mater. Res.* **2006**, *21*, 349.
(32) Holzapfel, V.; Musyanovych, A.; Landfester, K.; Lorenz, M. R.; Mailänder, V. *Macromol. Chem. Phys.* **2005**, *206*, 2440.
(33) Musyanovych, A.; Rossmanith, R.; Tontsch, C.; Landfester, K. *Langmuir* **2007**, *23*, 5367.
(34) Liu, D. P.; Majewski, P.; O'Neill, B. K.; Ngothai, Y.; Colby, C. B. *J. Biomed. Mater. Res., Part A* **2006**, *77A*, 763.

Table 1. Recipe for Miniemulsion Polymerization of Functionalized Latexes

ingredients	with ionic surfactant (g)	with nonionic surfactant (g)
styrene	6−5.82	6−5.1
acrylic acid	0−0.18	0−0.9
initiator (V59)	0.1	0.1
hexadecane	0.25	0.25
SDS	0.072	
Lutensol AT50		0.2
water	24	24

AT50 (or 72 mg of SDS). After 1 h of stirring for pre-emulsification, the miniemulsion was prepared by ultrasonication of the mixture for 120 s at 90% amplitude (Branson sonifier W450 Digital, $^1/_2$-in. tip) at 0 °C in order to prevent polymerization during the preparation. The copolymerization was performed at 72 °C for about 20 h. The latexes synthesized with nonionic surfactants were washed in order to remove free chains of poly(acrylic acid) if any, while the latexes prepared with the ionic surfactant SDS were dialyzed extensively to remove SDS as much as possible (conductivity of the washing water <6 μS/cm) in addition to poly(acrylic acid) in the aqueous phase. In the latter case, stability of the latexes was provided by adding about 0.8 wt % nonionic surfactant Lutensol AT50 containing aqueous solution by multiple centrifugation and redispersion.

Mineralization Using Polymeric Nanoparticles. For all the latexes, the amount of calcium and phosphate ions added for HAP formation was always the same. Loading of the particles was carried out by first adjusting the pH to 10 by use of 26% ammonia solution. The samples were stirred at 37 °C (as in our previous experiment[22]) and then loaded with calcium ions, followed by addition of phosphate ions as follows. For about 0.1 g of polymer, about 0.5 mmol of $Ca(NO_3)_2 \cdot 4H_2O$ was added, and then the samples were stirred for 2 h to allow binding of calcium ions. The phosphate solution [0.3 mmol of $(NH_4)_2HPO_4$] was added dropwise for about 1 h. The molar ratio of calcium to phosphate was maintained at 5:3 in all loadings. The samples were stirred after being loaded for about 24 h. The pH was maintained at 10 throughout the experiment. The samples were later washed and freeze-dried for further characterization.

Characterization Methods

Dynamic Light Scattering. Sizes of all the nanoparticles from a diluted dispersion were characterized by dynamic light scattering (DLS) on a Zetasizer Nano NS (Malvern Instruments), equipped with a detector to measure the intensity of the scattered light at 173° to the incident beam. The dynamic light scattering (DLS) measurements give a value called *Z*-average size (or cumulant mean), which is an intensity mean and the polydispersity index (PDI). The standard cumulant analysis is the fit of a polynomial to the log of the *G*1 correlation function given by

$$\ln(G1) = a + bt + ct^2 + dt^3 \qquad (1)$$

where t is the time.

The second-order cumulant b is converted to a size via the dispersant viscosity and instrumental constants. The coefficient of the squared term c, when scaled as $2c/b^2$, is defined as the polydispersity index (PDI). The calculations for these parameters are defined in the ISO standard document 13321:1996E. PDI is a measure of the particle size distribution and is a dimensionless number that describes the heterogeneity of the sample; it can range from 0 (monodisperse) to 1 (polydisperse).

Transmission Electron Microscopy. The nanoparticles were imaged on a Philips 400 TEM (Fei, Eindhoven, The Netherlands) operating at an accelerating voltage of 80 kV. All samples were prepared by air-drying the diluted sample on a carbon-coated copper grid without any additional contrasting. Most of the hybrid particles were characterized (before and after washing) prior to the freeze-drying step.

The hybrid polymer/HAP composite particles were also characterized on a Philips CM20 transmission electron microscope (dark field and bright field imaging modes) operating at 200 kV.

Scanning Electron Microscopy. For preparation of the loaded samples, a drop of the diluted dispersion was dropped on a Si wafer and left for air-drying. The samples were double-layer-coated by electron beam evaporation with 2 nm of platinum−carbon at an angle of 45° and 5 nm of carbon (perpendicular). The imaging was performed by use of the secondary electron signal on a Hitachi S-5200, in-lens field emission scanning electron microscope (SEM), (Hitachi, Tokyo, Japan). The beam current was 10^{-11} A and the primary accelerating voltage was 10 kV.

X-ray Diffraction. The freeze-dried samples obtained after loading with respective salt solutions were washed four times by resuspension in water and subsequent centrifugation at 14 000 rpm until they were finally freeze-dried again. These samples were characterized on a PANalytical X'Pert Pro diffractometer equipped with a multichannel detector by use of a Cu Kα ($\lambda = 0.154$ nm) monochromatic X-ray beam. All the samples were measured with a $\theta-2\theta$ configuration. The XRD reference pattern for hydroxyapatite (HAP) was calculated from the unit cell data of the crystals by use of the diffraction module in the MS modeling software (Accelrys).

Surface Charge Determination. The total solid content and styrene conversion were measured gravimetrically on a Kern RH 120-3 gravimeter. All latex samples were cleaned by repetitive centrifugation/redispersion in demineralized water prior to the measurement.

The surface charge density of the functionalized polystyrene latexes was determined by means of polyelectrolyte titration employing a particle charge detector PCD 02 (Mütek GmbH, Germany) in combination with a 702SM Titrino (Metrohm AG, Switzerland) automatic titrator. Carboxyl functional groups were titrated with 10^{-3} M polyelectrolyte standard, cationic poly(diallyldimethyl ammonium chloride) (PDADMAC), to determine the point of zero charge. The measurements were carried out with 10 mL of a cleaned latex sample in aqueous solution with a known solid content. The amount of charged groups per gram of latex particles was calculated from the consumed volume of polyelectrolyte (an average of at least three titrations) by use of the following equation:

$$(\text{groups}/g_{\text{polymer}}) = \frac{VMN_A}{SC} \qquad (2)$$

where V is the volume of consumed polyelectrolyte in liters, M is the molar concentration of polyelectrolyte in moles per liter, N_A is Avogadro's constant (6.022×10^{23} mol^{-1}), and SC is the solid content of the latex sample in grams. By use of the particle size determined by DLS, the amount of groups per particle or per square unit was calculated from the following equations:

$$(\text{groups/particle}) = (\text{groups}/g_{\text{polymer}})\frac{\rho D_z^3 \pi}{6} \qquad (3)$$

$$(\text{groups/nm}^2) = (\text{groups}/g_{\text{polymer}})\frac{\rho D_z \times 10^{-18}}{6} \qquad (4)$$

where D_z is the average diameter of the particle in nanometers and ρ is the density of polystyrene (1.045×10^3 g·L^{-1}).

Table 2. Characterization of Functionalized Latex Particles Obtained with Nonionic Surfactant Lutensol AT50

sample	Lutensol AT50 (mg)	comonomer AA (wt % on styrene)	solid content (%)	D_z (nm)	PDI
PSAA1	200	0	13.7	321	0.112
PSAA2	200	1	13.8	162	0.049
PSAA3	200	2	13.9	207	0.114
PSAA4	200	3	18.6	254	0.026
PSAA5	700	5	22.9	125	0.019

Thermogravimetric Aanalysis. The hydroxyapatite content in the hybrid particles was measured from the dried samples via thermogravimetry. Thermogravimetric analyses were performed with a Mettler-Toledo TGA/SDTA851e under nitrogen atmosphere. The temperature range was from room temperature to 1100 °C at a heating rate of 10 °C·min^{-1}.

Results and Discussion

Polymerization with Ionic and Nonionic Surfactants. The carboxyl-functionalized polystyrene particles were prepared by polymerizing styrene with different amounts of the functional comonomer acrylic acid (AA) via miniemulsion copolymerization. In all the polymerization processes, the oil-soluble initiator 2,2′-azobis(2-methyl butyronitrile), V59, was used in order to avoid the generation of free radicals in the aqueous phase, thereby preventing polymerization of the hydrophilic monomer in the water phase. Lutensol AT50 was used as a nonionic steric stabilizer, and SDS was used as an anionic electrostatic stabilizer. The polymerization was complete after 20 h in all runs. Table 2 shows the size of the particles as a function of the acrylic acid amount and the corresponding size distribution (PDI) measured by DLS, as well as the solid content of the resulting latexes that were prepared with Lutensol AT50. The diameters of the functionalized particles were smaller than the pure polystyrene particles, which is due to the hydrophilic nature of the acrylic monomer as reported earlier.[33] The oligomers or the polymeric chains of AA formed during the polymerization can also impart electosteric stabilization.[35,36] The latexes produced with the nonionic surfactant were found to be viscous at the end of the polymerization. Using 0.8% of Lutensol AT50 with respect to the continuous phase (200 mg of surfactant in 24 g of water), does not allow production of a stable latex with more than 3 wt % AA with respect to the total amount of monomer. Nevertheless, latexes with 5 wt % AA could be produced by use of high amounts of Lutensol AT50 of about 2.9% with respect to the aqueous phase (700 mg of surfactant in 24 g of water). The difficulties in producing latexes with increasing comonomer AA content might be attributed to the instability caused by bridging of the latex particles by the polymeric chains with increasing amount of AA and by the rapid polymerization of AA at low pH.[35] The increase in viscosity due to the water-soluble polymeric chains has already been reported to play a role under these conditions.[37] In addition, the specific interaction of ethylene oxide units of the nonionic surfactant with the carboxyl group, leading to a change in conformation of the ethylene oxide chains, can also possibly render the nonionic surfactant less effective as a stabilizer.[38−40]

In contrast to the nonionic surfactant, use of the low molecular weight anionic surfactant SDS (always 72 mg/sample) results in relatively less viscous latexes and allows the synthesis of latexes with higher amounts of AA content with low coagulum formation.[32,33] The high stability of the latexes could be attributed to the efficient electrostatic stabilization offered by SDS as compared to the steric stabilization in case of Lutensol AT50. Table 3 presents the characterization of the functionalized latexes prepared with SDS as surfactant. Here, the size of the latexes decreases only slightly with increasing AA amount.

From the solid contents, the yield of polymerization was about ∼90−100% for the low molecular weight surfactant compared to ∼50−90% for the nonionic polymeric surfactant. These values are similar to those reported earlier.[32,33]

As the aim of preparing these functionalized particles was to use them as templates for HAP growth, the ionic surfactant stabilized particles were dialyzed extensively to remove SDS, followed by exchanging the surfactant with 0.8% Lutensol AT50 aqueous solution by multiple centrifugation and redispersion processes. The particle size after exchange with Lutensol AT50 is also given in Table 3. The increase in particle size is due to the increase in hydrodynamic radius of the particles in the presence of a polymeric surfactant, although the size of the solid polymeric particles (the core) itself is not changed. It is necessary to bear in mind that such an additional steric stabilization allows stability against electrolyte addition. Henceforth, the loading with ions could be performed without impairing the colloidal stability.

Surface Group Titration. The amount of carboxyl groups present on the particle surface was quantified by polyelectrolyte titration after washing and, in the case where SDS was used in the synthesis, extensive dialysis followed by stabilization with Lutensol AT50. In the case of functionalized particles prepared with the nonionic surfactant Lutensol AT50, the charge arises only from the comonomer AA. In the case of latexes prepared with the ionic surfactant SDS, charges originating from sulfate groups of the SDS surfactant molecules as well as carboxyl groups of the functional monomer have to be considered. In the latter case, the surface carboxyl groups are usually determined as the difference between the amount of polyelectrolyte that is consumed during the titration at pH 2 and pH 10. At pH 2 only the sulfate groups are responsible for the charge, as all the carboxyl groups are protonated, while at pH 10 all the anionic groups are deprotonated.

Although the latexes prepared with SDS as surfactant were extensively washed, the charge originating at pH 2 indicated that there are still some residual SDS molecules in the washed latexes. The particle size used for surface charge estimation was the value measured before the surfactant

(35) Vorwerg, L.; Gilbert, R. G. *Macromolecules* **2000**, *33*, 6693.
(36) Polpanich, D.; Tangboriboonrat, P.; Elaïssari, A. *Colloid Polym. Sci.* **2005**, *284*, 183.
(37) Reynhout, X. E. E.; Meuldijk, J.; Drinkenburg, B. A. H. *Prog. Colloid Polym. Sci.* **2004**, *124*, 64.
(38) Romero-Cano, M. S.; Martin-Rodriguez, A.; de las Nieves, F. J. *Langmuir* **2001**, *17*, 3505.
(39) Romero-Cano, M. S.; Martin-Rodriguez, A.; de las Nieves, F. J. *Colloid Polym. Sci.* **2002**, *280*, 526.
(40) Liang, W.; Tadros, T. F.; Luckham, P. F. *Langmuir* **1994**, *10*, 441.

Table 3. Characterization of Functionalized Latex Particles Obtained by Use of 72 mg of Ionic Surfactant SDS

			particle size with SDS		particle size after dialysis and exchange with Lutensol AT50	
sample	comonomer AA (wt % on styrene)	solid content (%)	D_z (nm)	PDI	D_z (nm)	PDI
PSAA6	0	19.4	108	0.023	136	0.163
PSAA7	1	17.6	104	0.092	176	0.268
PSAA8	3	18.5	94	0.069	135	0.148
PSAA9	5	18.0	89	0.087	119	0.115
PSAA10	10	18.2	87	0.089	111	0.106

Table 4. Surface Charge Determination of Functionalized Latexes Prepared with Nonionic Surfactant and with Ionic Surfactant after Dialysis and Stabilization with Lutensol AT50

nonionic surfactant Lutensol AT50			ionic surfactant SDS (after dialysis and stabilization with Lutensol AT50)		
sample	COO^- groups per particle	COO^- groups per nm^2	sample	COO^- groups per particle	COO^- groups per nm^2
PSAA1			PSAA6		
PSAA2	161 851	1.97	PSAA7	13 172	0.39
PSAA3	416 089	3.10	PSAA8	13 230	0.48
PSAA4	883 263	4.35	PSAA9	31 401	1.25
PSAA5	265 292	5.44	PSAA10	37 437	1.59

Scheme 1. Schematic Illustration of HAP Formation on a Carboxyl-Functionalized Polymeric Nanoparticle by Addition of Ca^{2+} and PO_4^{3-} Ions

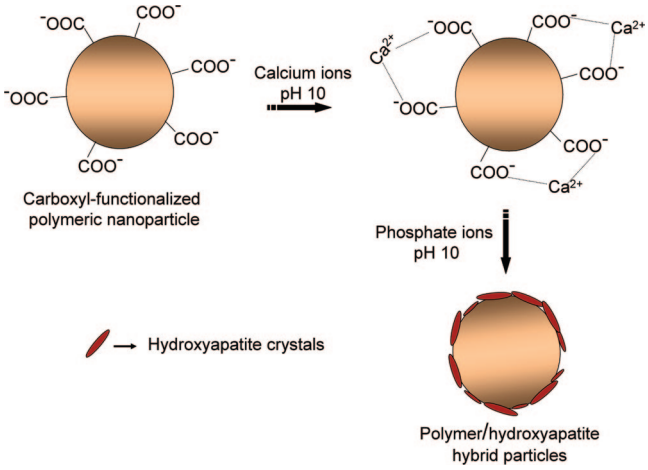

exchange, as the carboxyl groups are covalently bound to the surface or closely linked to the surface (in the case of a hairy layer) of the particles and, in addition, the residual SDS molecules, which also give rise to charge, are located close to the particle surface owing to their size. Therefore, the particle size prior to Lutensol AT50 addition and after some dialysis (washing water conductivity of about 25 μS/cm) was used. The density of the surface charge for the latexes is presented in Table 4.

It can be seen that there is a clear tendency of increasing number of charge groups with increasing AA content. Also, it can be observed that, for the same acrylic acid content, the average surface charge density of carboxyl groups for particles prepared with Lutensol AT50 is higher than for particles prepared with ionic surfactant SDS. This can be attributed mainly to the competition of SDS with AA on the surface owing to their ionic nature.

Formation of Hydroxyapatite Nanocrystals. HAP formation on the surface of the functionalized particle was performed as shown schematically in Scheme 1. The addition of calcium ions followed by a dropwise addition of phosphate ions, corresponding to the stoichiometric Ca^{2+}:PO_4^{3-} ratio for hydroxyapatite [$Ca_{10}(PO_4)_6(OH)_2$] formation, at constant pH of 10 leads to the generation of hybrid particles. The latexes prepared with different amounts of AA and different surfactant types were always loaded with a fixed concentration of the respective ions for HAP formation, and comparative characterizations were performed by SEM, TEM, and XRD.

For all the latexes prepared with SDS as surfactant, calcium and phosphate ions were added after dialyzing and stabilizing with Lutensol AT50. HRSEM images showing the varying amounts of crystals formed on the particles as a function of different amounts of acrylic acid are presented in Figure 1.

The amount of inorganic crystals formed on the surface of the particles directly correlates with the amount of functional groups present on the surface. Although the samples were washed extensively in order to remove the SDS, it was not possible to remove the SDS completely (known from the surface group titration). For the sample with 0 wt % AA (PSAA6) in Figure 1a, although the charge arises only from the residual anionic surfactant, the absence of HAP formation on the surface of the particle indicates that either the residual amount of SDS is not sufficient or the carboxyl groups are necessary for the HAP nucleation. The latter reason also points toward the previous studies made with SAMs, where the -COOH groups were found to be the optimum candidate for HAP formation.[34]

For comparison, all the latexes prepared with different AA contents and nonionic surfactant were loaded with the same respective amounts of calcium and phosphate ions in the stoichiometric ratio for HAP formation as in the case of latexes prepared with SDS as surfactant. The hybrid particles are presented in Figure 2b−d. As reference, a sample with 0 wt % AA (PSAA1) where no hybrid particles are formed is presented in Figure 2a.

It can be seen that the reference sample containing 0 wt % AA (PSAA1) in Figure 2a has no crystal on its surface, which clearly proves that the crystals are formed only because of carboxyl functionalization. As before, the amount of crystals formed on the surface of the particles clearly increases with increasing number of surface functional groups. Also, it can be very well evidenced from these images that, for the same amounts of AA, surface coverage of the particles by the formed crystals is much more

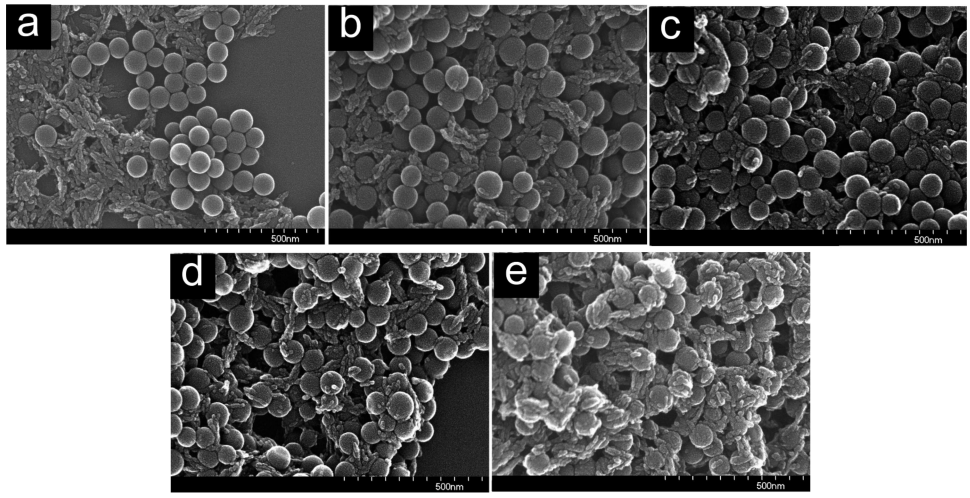

Figure 1. (a−e) HRSEM images illustrating HAP formation for samples prepared by use of ionic surfactant (SDS) with (a) 0 wt % AA (sample PSAA6), (b) 1 wt % AA (sample PSAA7), (c) 3 wt % AA (sample PSAA8), (d) 5 wt % AA (sample PSAA9), and (e) 10 wt % AA (sample PSAA10).

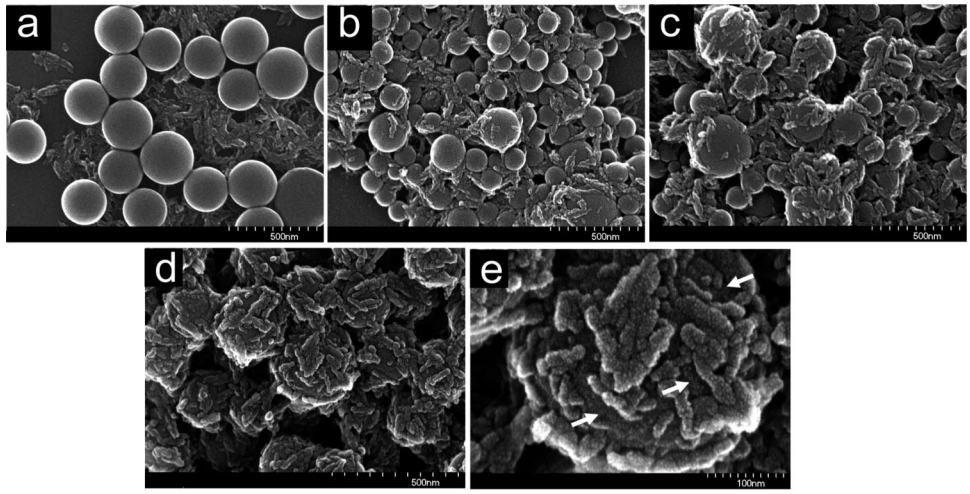

Figure 2. (a−e) HRSEM images illustrating HAP formation for samples prepared by use of nonionic surfactant (Lutensol AT50) with (a) 0 wt % AA (sample PSAA1), (b) 1 wt % AA (sample PSAA2), (c) 2 wt % AA (sample PSAA3), and (d) 3 wt % AA (sample PSAA4). (e) The particle in panel d is shown at higher magnification to see the surface coverage. Arrows indicating the underlying polymeric core nanoparticle show that complete coverage of the surface with the crystals is not yet achieved.

pronounced for these particles as compared to those prepared with SDS. However, even with the highest coverage of the particle by HAP crystals (Figure 2d,e), it is still possible to see the underlying polymeric core nanoparticle in high magnification (arrows in Figure 2e), indicating that the complete coverage of the surface with the crystals is not yet achieved.

TEM characterization of the hybrid particles prepared with latex PSAA4 (3 wt % AA) is shown in Figure 3. The two images were taken from the same sample before and after washing to show that the washing procedure does not remove the HAP nanocrystals on the surface and the formed crystals are strongly bound to the surface. In Figure 4, bright-field (BF) and corresponding dark-field (DF) images of an enlarged area from the same sample after washing are presented. With the BF image, one can clearly see the incomplete surface coverage of the hybrid particles, as observed in the HRSEM image in Figure 2e, and in the DF image, one can clearly see that the formed inorganic material is crystalline in nature and the crystals present on the surface of the particles are oriented in different directions.

It was found that for a high comonomer content of 5 wt % AA (sample PSAA5), shown in Figure 5, there were only a few crystals grafted on the surface. Although the sample was prepared with more AA content and the same surfactant type (Lutensol AT50), this sample cannot be directly compared with the other samples prepared with the same surfactant type as they were synthesized with a low fixed Lutensol AT50 concentration (two parameters have been varied at the same time, that is, the amounts of AA and surfactant). However, the high amount of carboxyl groups, which was found to be more in the case of latex prepared with 5 wt % AA (5.4 COOH groups/nm^2), did not play a significant role in HAP formation as in the case of latex prepared with 3 wt % AA (4.4 COOH groups/nm^2). Such a reduction in the formation of HAP crystals on the surface in spite of high availability of the carboxyl groups can be attributed to the reason that these particles were prepared with relatively large amounts of nonionic surfactant (3.5 times more than the other latexes prepared with Lutensol AT50), which could possibly shield the functionalized surface from participating in crystal formation. As a result of this

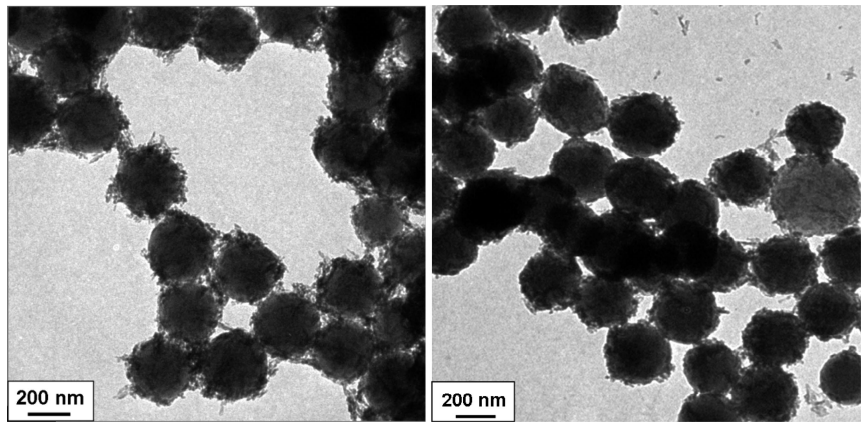

Figure 3. TEM images from hybrid particles prepared from sample PSAA4 before (left) and after washing (right).

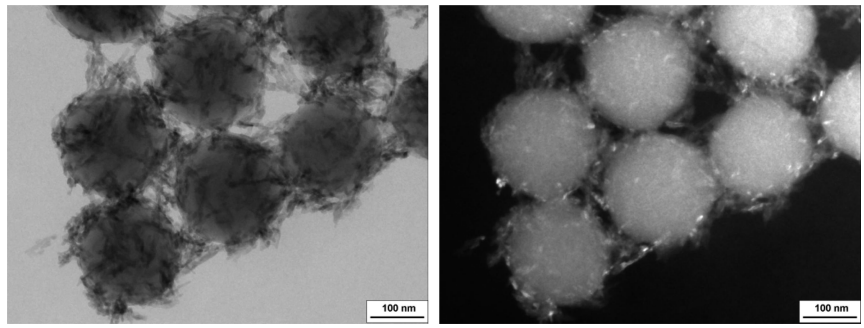

Figure 4. TEM images from hybrid particles, prepared from sample PSAA4 after washing, in bright-field (left) and dark-field (right) imaging modes.

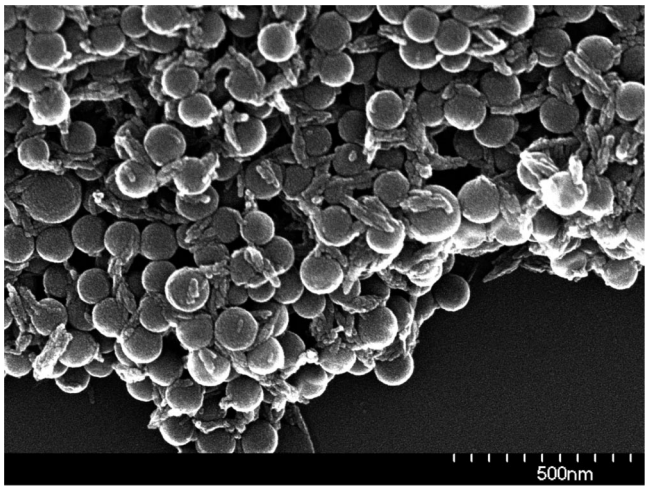

Figure 5. HAP formation with 5 wt % AA (sample PSAA5).

screening of the carboxyl groups, most of the particles were found bare without crystals. Thus, it is absolutely necessary to have an optimum surfactant concentration, in addition to high carboxyl functionalization on the surface of the particles, for high HAP nanocrystal formation.

A common aspect that can be seen in the latexes prepared with both surfactant types is that even for highly carboxyl-functionalized particles apart from surface-bound HAP, small amounts of bulk precipitated HAP crystals are also present. Although this occurs at pH 10, where all the carboxyl groups are deprotonated and can bind Ca^{2+}, it is possible that at these high pH values and concentration the driving force for HAP nucleation and its growth is too strong and above the level at which nuclei can spontaneously form in bulk solution. The bulk-precipitated crystals also have the possibility to precipitate on the particle surface apart from aggregating into large agglomerates. Formation of a high amount of nanocrystals on the surface of the particles leads to decreased mobility of the polymeric stabilizer as well as to increased density of the hybrid particles, thereby proving detrimental to colloidal stability. The problem of bulk precipitation can be solved by optimizing the parameters during the loading procedure. One possible way could be by controlling the amount of ions added and adopting several steps of ion addition during the loading of the functionalized particles. The amount of calcium ions added should be controlled simultaneously by titrating the carboxyl groups available and then subsequently adding the required phosphate ions corresponding to the concentration of complexed calcium ions for HAP formation. This could be followed by slow addition of a second sequence of calcium and phosphate ions for further growth of HAP on the already existing hydroxyapatite crystals. The latter step might also improve the surface coverage of the hybrid particles. The problem of colloidal instability could be solved by performing poststabilization of the hybrid particles by addition of a suitable surfactant.

The hybrid particles prepared with both surfactant types were washed well by multiple centrifugation and redispersion in demineralized water to remove the ammonium nitrate formed as a byproduct and then freeze-dried prior to XRD characterization. XRD patterns for all the hybrid particles prepared with nonionic and ionic surfactants, along with XRD patterns from the dried unloaded polymeric latexes to show the influence of the polymeric template, are presented

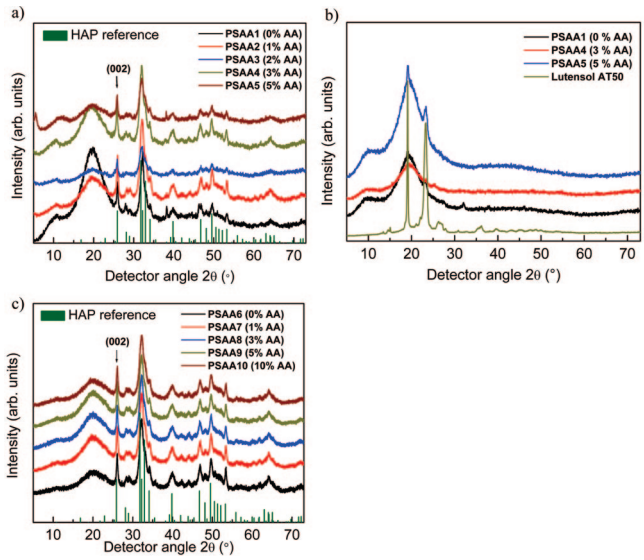

Figure 6. XRD patterns (a) from hybrid particles prepared from latexes synthesized with nonionic surfactant (Lutensol AT50), (b) from pure polymeric particles (without HAP) prepared with nonionic surfactant (Lutensol AT50) to show the influence of polymeric template patterns, and (c) from hybrid particles prepared from latexes synthesized by use of ionic surfactant (SDS). The samples before loading were dialyzed and then stabilized with Lutensol AT50.

in Figure 6. The diffraction patterns of the dried unloaded polymeric latexes are presented for the samples with 0, 3, and 5 wt % AA in the case of latexes prepared with nonionic surfactant in order to show the influence of the polymeric template with varying AA content. As the samples prepared with SDS as surfactant were excessively dialyzed and then stabilized with Lutensol AT50, similar peaks corresponding to Lutensol AT50 were observed in those samples. Hence, the XRD scans of the unloaded polymeric nanoparticles in the latter case are not shown here.

XRD characterization of these samples clearly proves that the formed crystals are crystalline hydroxyapatite. From XRD characterization, it can be seen that all the characteristic peaks of HAP as shown in the reference pattern are present in the samples. The sharp peaks clearly illustrate the crystallinity of the crystals present. The average crystallite size estimated from the (002) reflection (indicated by an arrow in the diffractogram) of the XRD scans by use of the Scherrer equation was between 19 and 22 nm. Apparently the size of the crystallites does not depend on the nucleation site, as they are the same on the particle and in the solution. Thermogravimetric analysis on the hybrid particles from the samples showed that about 30−33 wt % HAP was formed, which was in accordance with the theoretical value (33.3 wt %) calculated for HAP formation for full conversion.

Conclusion

It was shown that the miniemulsion technique offers a very simple route to prepare carboxyl-functionalized latex particles with different amounts of comonomer, acrylic acid, and surfactant types. Nonionic surfactant was efficient in preparing carboxyl-functionalized particles with a high surface charge density with low amounts of the comonomer AA. The functionalized particles were successfully exploited as templates for hydroxyapatite formation. It was found that, for a fixed concentration of Ca^{2+} and PO_4^{3-} ions added, the amount of HAP formed on the surface of the particles increased with increasing AA amount. The absence of HAP on latexes prepared with 0 wt % AA for both ionic and nonionic surfactant types confirms that the amount of HAP formed depends only on the amount of carboxyl groups present on the surface. It was found that HAP formation was well pronounced for particles prepared with nonionic surfactant, which is in agreement with the high amount of -COOH groups as compared to the latexes prepared with SDS as anionic surfactant. However, it was also found that, in addition to high carboxyl functionalization on the surface of the particles, it is absolutely necessary to have an optimum surfactant concentration for particles prepared with nonionic surfactant to obtain high HAP nanocrystal formation.

Such hybrid nanoparticles with HAP crystals on the surface have great potential in the field of tissue engineering. They could be finally used for the coating of implants in order to make them more osteoconductive as well as for the preparation of scaffolds for tissue engineering. Moreover, as the ease of encapsulation of inorganic materials and fluorescent markers (which can be treated as model drug substance) with high efficiency is a well-known trait for the versatile miniemulsion technique,[41] it allows one to load the polymeric nanoparticles with bioactive molecules and drugs. Such incorporation of bioactive substances into the nanoparticle formulation, in addition to employing a suitable biodegradable polymeric nanoparticle, facilitates the release of growth factors and antibiotics to better treat bone defects and support wound healing. This biomimetic approach of using surface-functionalized nanoparticles as templates in aqueous phase reported here can be very well extended to other crystallization processes to produce interesting hybrid materials for a wide range of technological applications.

Acknowledgment. We thank S. Blessing of the Institute of Inorganic Chemistry I, University of Ulm, for the XRD measurements; A. Chuvilin of the Electron Microscopy Group of Material Science, University of Ulm, for the characterization via Philips CM20 TEM; and Professor Dr. Paul Walther for his expertise in electron microscopy and Mr. E. Schmidt for help in the sample preparation in the Central Facility for Electron Microscopy, University of Ulm.

CM9001724

(41) Holzapfel, V.; Lorenz, M.; Weiss, C. K.; Schrezenmeier, H.; Landfester, K.; Mailänder, V. *J. Phys.: Condens. Matter* **2006**, *18*, S2581.